Automotive Paint Permittivity Estimation in Low-THz frequency

Y. Xiao, F. Norouzian, E. G. Hoare, A. Bystrov, M. Gashinova, M. Cherniakov

***Abstract*- The propagation characteristics of radar signal through vehicle infrastructure depends on electro-physical properties of a media, in particularly complex permittivity of automotive paint. In this paper, complex permittivities of various automotive paints are measured within the range from 0.14 THz to 1.1 THz using Terahertz Vector Network Analyzer (THz-VNA). The measured complex permittivities are then used to evaluate the attenuation and reflectivity of aggregate multi-layer paint.**

Keywords— Low-THz automotive radar, signal propagation, dielectric constant, THz technology, THz-Vector Network Analyzer

I. INTRODUCTION

Automotive radar has become a key technology for developing advanced driver assistance systems (ADAS). Currently, various vehicle external radar sensing features are available on the market, such as side impact detection, blind spot warning, pre-crash, lane change aid and collision avoidance, in addition to ACC [1]. Increasing number of sensors, as well as demand for more advanced features, able to provide higher levels of automations lead to pressing need of further miniaturization of sensors, capable to deliver high information content for both radar and communication functionalities [2] The low-terahertz (Low-THz), or alternatively, sub-THz radar is a promising candidate for the next generation of automotive radar, taking advantages of smaller packaging and the increase in the radar signal bandwidth and, therefore, is becoming a development trend .

Before launching Low-THz radars into the automotive market, it is however required to investigate viability of incorporating Low-THz radar into vehicle infrastructure whilst maintaining compatibility with vehicle manufacturer styling and packaging requirements, without compromising the performance of the sensors [3].

The knowledge of the complex permittivity (CP) of materials, in particularly paint layers and substrate, is crucial to evaluate impact of the radar surrounding and enclosure on sensing performance . The estimations of dielectric constant of automotive paints and the effects of attenuation and reflection caused by paint layers have been investigated at 79 GHz in [4, 5]. In [6], the authors presented the study on the modelling of attenuation in vehicle infrastructure (various bumper samples with multiple layers of paints and headlight cover) at three frequency bands around 77, 300 and 670 GHz, which requires knowledge of material electric properties. Current paper concerns with methodology of measurement of CPs of automotive paints within the wide range of frequencies from 0.14 to 1.1 THz using VNA [7]. The measured CPs are then used for the modelling of attenuation and reflection within multi-layer vehicle infrastructure.

I. THEORETICAL MODEL

CP is the fundamental electrical property of a material, can be considered as measure of capacitance to form an electric field in a medium made of the material [8] and is dependent on frequency of the EM field: $\varepsilon(f)=\varepsilon'-j\varepsilon''=\varepsilon_0(\varepsilon'_r-j\varepsilon''_r)$. The real part ε' represents the ability of the medium to store the electromagnetic (EM) energy when signal passes through it, and the imaginary part ε'' represents the degree of EM energy attenuation inside the material [9].

The ray diagram of the process of propagation through the flat sample is shown in Fig. 1. At each air-medium interface, the incident field, E_{in} , is split into a transmitted and a reflected fields, E_{trans} and E_{refl} , respectively. The multiple reflections inside the sample from each interface are formed giving rise to a periodic Fabry-Perot (FP) reflections [10]. The notation used in Fig. 1 are defined in the Table I.

TABLE I. NOTATION LIST

Symbol	Definitions and Descriptions
ω	angular frequency
l_a, l_s	thickness of air and paint sample, respectively
$\varepsilon_0, \varepsilon_a, \varepsilon_s$	permittivity of vacuum, air, paint sample, respectively
μ_0, μ_a, μ_s	permeability of vacuum, air, paint sample, respectively
δ_a, δ_s	conductivity of air, paint sample, respectively $\delta_s=\omega\varepsilon_s''\varepsilon_0$
k_a, k_s	wave number of air, paint sample, respectively $k_s=\omega\sqrt{\varepsilon_0\varepsilon_s\mu_0}$.
$E_{in}, E_{trans}, E_{refl}$	incident signal, transmitted signal and reflected signal
P_a, P_s	propagation coefficient through air, paint sample, respectively. The latter is defined as $P_s=\exp(-j\omega\sqrt{\varepsilon_0\varepsilon_s\mu_0}l_s)$.
η_a, η_s	wave impedance of air, paint sample, respectively
N	number of FP reflections inside the medium
r_{as}, r_{sa}	reflection coefficient at the interfaces of air-sample, sample-air, respectively
t_{as}, t_{sa}	transmission coefficient at the interfaces of air-sample, sample-air, respectively

We will use the transmissivity as a parameter characterizing transmission through the material of interest. The transmissivity through the sample with interfaces 'air-sample' (input interface) and 'sample-air' (output interface) after N times FP reflections can be defined as in [11, 12]:

$$T_{cal} = \left|\frac{E^s_{trans}}{E^r_{trans}}\right|^2 = \left|t_{as}t_{sa}P_s + t_{as}t_{sa}r_{as}r_{sa}P_s^3 + \ldots + t_{as}t_{sa}(r_{sa}^2)^N P_s^{(2N+1)}\right|^2$$

$$\xrightarrow{N\Rightarrow\infty} \left|\frac{t_{as}t_{sa}P_s}{1+r_{as}r_{sa}P_s^2}\right|^2 \quad (1)$$

where E^r_{trans} is the transmitted electric field through the reference sample which is the sample holder without sample present, E^s_{trans} is the transmitted electric field through the sample after N times FP reflections [10, 13]. The transmission and reflection coefficients for a EM waves with wave impedance $\eta_s = \sqrt{\frac{j\omega\mu_s}{\delta_s + j\omega\varepsilon_0\varepsilon_s}}$ can be obtained using approach based on Fresnel's equations :

$$r_{as} = \frac{\eta_a\cos\theta_s - \eta_s\cos\theta_a}{\eta_a\cos\theta_s + \eta_s\cos\theta_a}, t_{as} = \frac{2\eta_a\cos\theta_s}{\eta_a\cos\theta_s + \eta_s\cos\theta_a} \quad (2)$$

$$r_{sa} = \frac{\eta_s\cos\theta_a - \eta_a\cos\theta_s}{\eta_s\cos\theta_a + \eta_a\cos\theta_s}, t_{sa} = \frac{2\eta_s\cos\theta_a}{\eta_s\cos\theta_a + \eta_a\cos\theta_s} \quad (3)$$

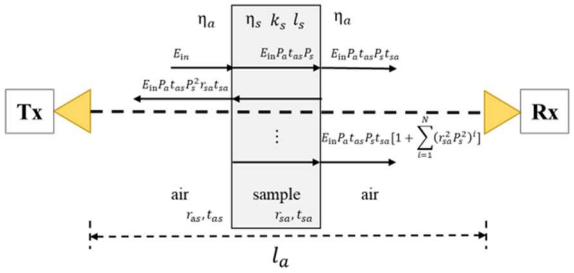

Fig. 1 Schematic of the electric fields of THz waveform through medium with one-layer structure.

Therefore when transmissivity for a particular medium is measured and calculated, the permittivity can then be evaluated by minimization of the root mean square error (RMSE) between them [10]. The approaches to measure transmissivity will be explained in the following sections of III.C, and III.E.

II. Experimental Methodology

A. Automotive paint sample structure

Automotive paint coating is an important part of the vehicle manufacturing process to give a smooth, glossy or sparkly look and also, to protect vehicle from UV radiation and corrosion [14, 15]. Automotive paint is usually applied in three coating layers: primer, basecoat and, finally, the clear coat layer. The thickness of each layer is around tens of micrometers.

The primer layer provides better adhesion of basecoat paint and the clear coat layer is used for protecting basecoat paint from scratch and erosion due to weather. It is actually the basecoat which define the color and look and is typically made of either of three paints: solid paint, metallic paint and pearlescent paint (mica). Nowadays, metallic and mica colors are used more frequently and such paints contain aluminium or mica flakes (in the order of a few micrometers which is a small scattering particle compared with wavelength), respectively.

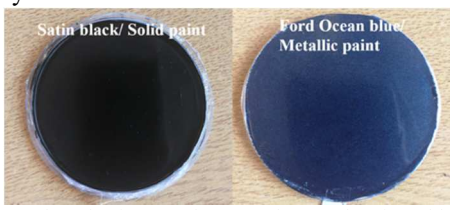

Fig. 2. Examples of paint samples (sample A and M in Table II, section III A) after drying. The presented colors are solid black and metallic blue.

Primers are typically red, white and grey to match the color of basecoat and the latter is used for the basecoats with dark colors such as blue, grey and black.

In our experiment, the liquid paints of all three basecoat types (solid, metallic and pearlescent) in various colors, primer in three colors (red, white and grey) and clear coat were used for producing the paint samples. To fabricate the paint samples for test, the liquid paint is poured onto a cling-film framed on a hoop, and, then, placed horizontally to dry. After seven days of drying, the samples of paint with the cling film were taken off from the hoop. The cling film has a negligible effect to permittivity measuring with the electrical thickness of several micrometer. Two paint samples are shown in Fig. 2 as the examples.

Table II presents samples fabricated based on method described in section III A, and their thickness measured by calipers.

TABLE II. Measured Thickness of Automotive Paint

No.	Paint class	l_c / μm
A	Satin black/ Solid paint	670
B	Tool Box red/ Solid paint	530
C	Dark Green/ Solid paint	510
D	Domestic Gloss White/ Solid paint	430
E	Dark Blue/ Solid paint	440
F	Volkswagen Grey Anthracite/ Pearlescent paint	260
G	Land Rover Epsom Green/ Pearlescent paint	410
H	Land Rover Oslo Blue/ Pearlescent paint	550
I	Renault Black/ Pearlescent paint	260
J	Peugeot Diablo Red/ Pearlescent paint	600
K	Audi Glacier White/ Metallic paint	940
L	Hyundai Phantom Black/ Metallic paint	370
M	Ford Ocean blue/ Metallic paint	570
N	BMW sparkling Graphite/ Metallic paint	970
O	Ford Tango Red/ Metallic paint	630
P	Gold/ Metallic paint	200
Q	Silver/ Metallic paint	200
R	Grey primer	420
S	White primer	1100
T	Red primer	630
U	Clear coat	670

B. *Experimental setup using THz-VNA*

The THz-VNA, Keysight PNA-X [16], at Low-THz frequencies, is equipped with six sets of up- and down-converters which cover the whole frequency range of 0.14 THz-1.1 THz. Transmission mode method [3] searches the CP by comparing and fitting the calculated transmissivity to the measured transmissivity. The experimental setup is shown in Fig. 6. Sections of waveguides are used as the antennas for each frequency range. The characteristic of waveguides and the calculated far field distances are listed in Table III.

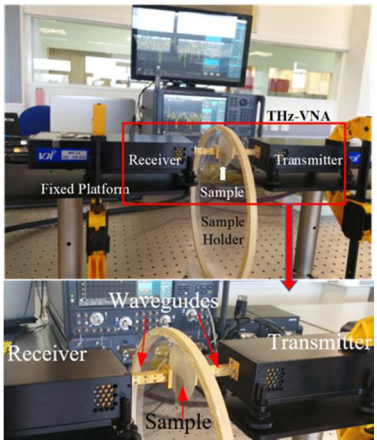

Fig. 3. Transmission measurement setup using THz-VNA.

The transmitter and receiver are aligned to maximize received power. The VNA is calibrated before each measurement to prevent the error caused by the change of environment. The sample of automotive paint is held between tightly stretched layers of the cling film, orthogonally to the line-of-sight. The distance between two waveguide antennas is 30 mm, to guarantee operation in the far field of antennas. The beamwidth of the waveguide antenna is around 60°. The illuminated area on the sample is of the diameter less than 20 mm.

TABLE III. THE APERTURES AND FARFIELD DISTANCES OF WAVEGUIDES IN DIFFERENT FREQUENCY RANGES.

Waveguide	Frequency (GHz)	Aperture ($mm \times mm$)	Farfield ($\geq mm$)
WM1295	140-220	1.295/0.6475	2.46
WM864	220-325	0.864/0.432	1.64
WM570	325-500	0.57/0.285	1.083
WM380	500-750	0.38/0.19	0.722
WM250	750-1100	0.25/0.125	0.458

C. *Estimation of complex permittivity by using VNA setup*

The transmissivity is defined as the ratio of power received in presence of sample to the one without the sample:

$$T_{mea}^{VNA} = \left| \frac{S_{21}^{s}}{S_{21}^{r}} \right|^2 \tag{4}$$

where S_{21}^{s}, S_{21}^{r} are the measured scattering coefficients with and without sample, respectively. The S_{21}^{r} is measured with the sample holder presented in the path.

The CP is determined by minimization of the difference between the measured transmissivity T_{mea}^{VNA} and calculated transmissivity T_{cal}, defined by (1):

$$D(\varepsilon',\varepsilon'') = \sum_{i=1}^{M} \left| T_{mea}^{VNA}(f_i) - T_{cal}(f_i,\varepsilon',\varepsilon'') \right| \tag{5}$$

where f_i is frequency of microwave signal in the range of 0.14 THz-1.1 THz, M is the number of frequency samples where transmissivity is measured. Therefore, the CP is calculated by root searching to provide the minimum value of D integrated over the whole considered frequency range.

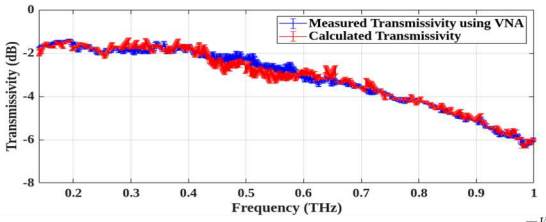

Fig. 4 Comparison of the measured transmissivity from VNA, (T_{mea}^{VNA}), and the calculated transmissivity T_{cal} which is closest to T_{mea}^{VNA}.

Fig. 4 presents the comparison between calculated T_{cal} and VNA, T_{mea}^{VNA}, of sample K. The T_{cal} is calculated based on Eq. (1) and the CP of sample K obtained by VNA setup is plotted in Fig. 7. T_{mea}^{TDS} is determined as:

$$T_{mea}^{TDS} = \left| \frac{S_s(f)}{S_r(f)} \right|^2 \tag{6}$$

The error bar in the figure represents the measurement standard deviation (STD) of three realizations. The plots of T_{mea}^{VNA} and T_{cal} show a reasonably good agreement.

III. EXPERIMENTAL RESULTS

In this section, the CP of automotive paints, listed in Table II, are measured and results are discussed.

A. *Measured dielectric properties of automotive paints*

The CP of paints measured at 79 GHz, which is current automotive standard frequency, can be found in [4, 5], and some typical values are shown in Table IV.

TABLE IV. CPS OF PAINT LAYERS AT 79 GHZ [4, 5].

Primer $\varepsilon'/\varepsilon''$	Clear coat $\varepsilon'/\varepsilon''$	Solid $\varepsilon'/\varepsilon''$	Pearlescent $\varepsilon'/\varepsilon''$	Metallic $\varepsilon'/\varepsilon''$
9/0.06	3.5/0.1	9.9/0.91	5.9/1.61	3.2/0.007

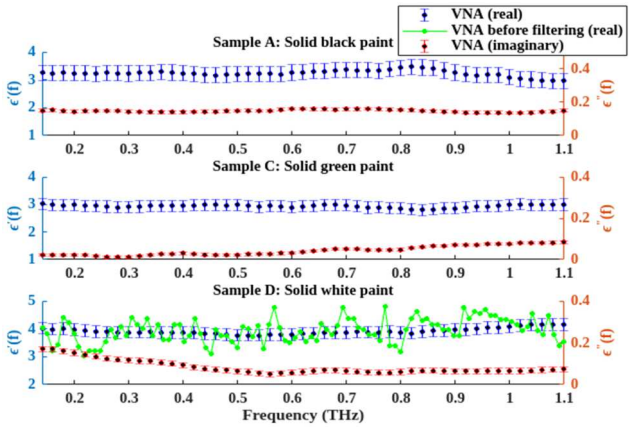

Fig. 5. Measured CP of solid automotive paints using THz-VNA.

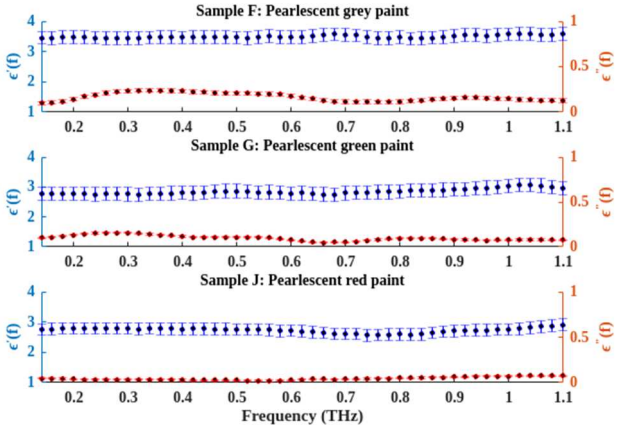

Fig. 6 Measured CP of pearlescent automotive paints using THz-VNA.

For all samples shown in Table II, the CP results at Low-THz are obtained using THz-VNA transmission measurement. The results are processed by applying the filter to remove fluctuations of the measured CP with frequency as will be explained below. Part of the measured CP values of solid paints, pearlescent paints, metallic paints and both primer and clear coats are shown in Fig. 5, 6, 7 and 8, respectively. For the unpresented samples, they have close CP performance to at least one of the existed samples. These figures are sharing the same legend as shown in Fig. 5. The bluelines and solid black lines represent the real part of CP, ε' (left y-axis), and the red plots and dashed black lines are for the imaginary part, ε'' (right y-axis).

The only dotted green line in Fig. 5 shows an unprocessed measured ε' by VNA for the sample D, as an illustration of fluctuating trend with frequency observed for all samples. It is expected, however, that for non-polar materials the dielectric constant does not change significantly with frequencies unless anomalous dispersion points are encountered. Such behavior is likely caused by the following possible issues of (1) calibration is not completely rigorous, (2) scattering, (3) sample has non-uniform thickness, therefore ε' and ε'' obtained by VNA were filtered over the whole frequency range, where within a sliding window of specific length the average of the permittivity is calculated. The number of samples contained in each window corresponds to the frequency band of 0.16 THz. We determine the filtering frequency band by observing the common period of fluctuation on measured CPs based on the FFT transformed value of original CPs from VNA.

The ε' of five considered solid paints (Fig. 5) is in the range of 2.5—4. The ε'' obtained from VNA is less than 0.4 in the frequency band of 0.14 THz-1.1 THz, and bigger variation is observed at lower frequency band. The black solid paint shows the largest ε'' value as well as larger increase with frequency, indicating higher losses compared to other solid paints, especially at higher frequencies.

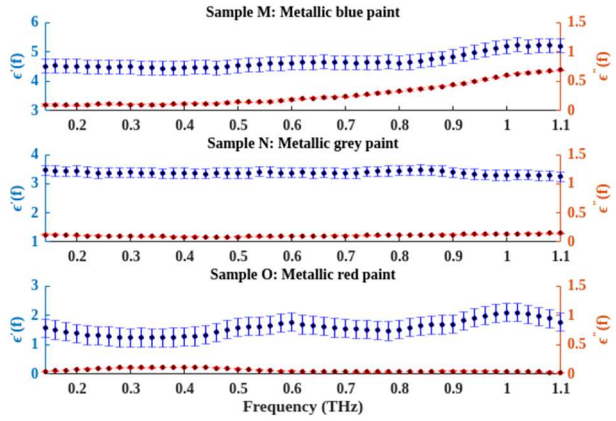

(a)

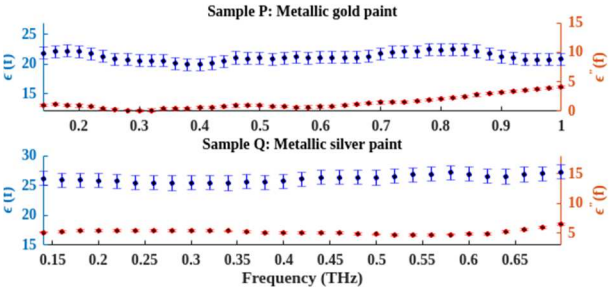

(b)

Fig. 7 Measured CP of metallic automotive paints using THz-VNA. (a) Results of metallic paints in color of red, white, black, blue and grey. (b) Results for bright gold and silver metallic paints.

The ε' of pearlescent paints (Fig. 6) is in the range of 2.6—3.6, while ε'' is slightly higher, than in case of solid paints. Similar to the case of solid paints, highest loss is observed for pearlescent grey and black paint which reaches at 2.0.

Results for seven metallic paints are shown in Fig. 7. However, the dielectric constants and losses of two metallic paints - in bright gold and silver (Fig. 7 (b)), are significantly different from other metallic paints (Fig. 7 (a)). Indeed the real and imaginary parts of CP of the metallic paints in Fig. 7 (a)

are in the range of 1.6—5.1 and 0.01—0.7, respectively, whereas, the real and imaginary parts of CP of the bright gold (sample P) and silver (sample Q) mantellic paints are in the range of 20—28 and 1.1—5, respectively. This is expected result due to higher concentration of metal for these two samples, which was also discussed in [4]. It is worth stressing that the permittivity of the metallic silver are only shown in frequency range of 0.14 THz—0.7 THz due to the higher attenuation caused by the sample so that the received signal power is close to the noise floor of VNA system.

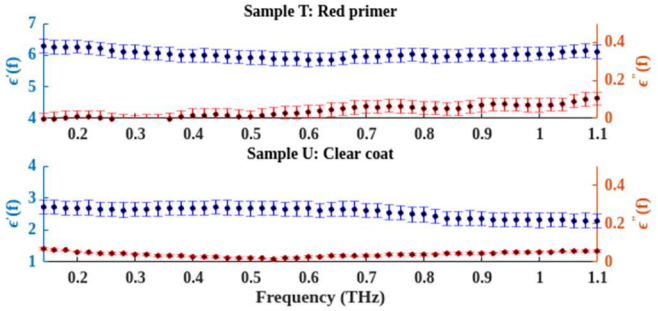

Fig. 8 Measured CP of primers in color of white, red and grey and clear coat based on THz-VNA setups.

The measured CP of clear coat and primers of three colors are shown in Fig. 8. The measured values of ε' of primer materials are around 5.08—6.28, while ε'' is basically below 0.22. Clear coat has ε' around 2.6 and the ε'' is below 0.1.

Higher measured dielectric loss and larger increase is observed in the results of the paint samples with darker colors in our selected samples. Analysis of effect of exact chemical composition of the paint on electric properties of paints is outside the scope of this paper, which only gives analysis of measurement techniques. The ε'' of majority of the paint samples show an increase with the frequency, indicating higher loss at higher frequencies, while the dielectric constant, ε', is mostly flat throughout the whole frequency range.

The measured CPs are summarized in Table IV, which shows the ranges over the whole frequency bands 0.14 THz-1.1 THz of VNA. For the other paint samples except metallic silver and golden ones, the standard deviation for ε' is less than 0.31, and for ε'' is less than 0.034. For the silver and golden ones, higher standard deviations are observed that ε' reached at 1.19, and ε'' reached at 0.19.

IV. Application to Practical Multi-Layer Automotive Structures

In this section, we analyze the attenuation and reflection of the signal in multi-layered paints. The measured CP values presented above are used for calculation. The theoretical model for calculating the transmissivity and reflectivity of multi-layer medium has been described in detail in our previous work [6].

TABLE V. Summary of the Measured CP and the Obtained Standard Deviation.

Sample	ε_r'	ε_r''	STD $\varepsilon_r'/\varepsilon_r''$	Sample	ε_r'	ε_r''	STD $\varepsilon_r'/\varepsilon_r''$	Sample	ε_r'	ε_r''	STD $\varepsilon_r'/\varepsilon_r''$
A solid	2.96-3.46	0.13-0.16	0.27/0.008	H Pearl	2.88-3.22	0.06-0.17	0.21/0.005	O Metallic	1.23-2.1	0.027-0.12	0.31/0.0038
B solid	2.40-3.05	0.04-0.09	0.23/0.006	I Pearl	3.24-3.55	0.1-0.31	0.21/0.02	P Metallic	19.9-22.5	0.002-4.7	1.02/0.19
C solid	2.80-3.03	0.01-0.84	0.2/0.005	J Pearl	2.56-2.96	0.01-0.076	0.18/0.007	Q Metallic	25-29	4.67-9.2	1.19/0.16
D solid	3.77-4.15	0.04-0.17	0.21/0.013	K Metallic	3.4-3.6	0.026-0.12	0.19/0.008	R Primer	4.9-5.2	0.07-0.23	0.21/0.014
E solid	2.80-3.25	0.01-0.96	0.22/0.008	L Metallic	2.3-2.7	0.069-0.13	0.21/0.007	S Primer	5.3-5.6	0.074-0.19	0.21/0.01
F Pearl	3.4-3.6	0.09-0.23	0.21/0.019	M Metallic	4.4-5.2	0.093-0.7	0.23/0.013	T Primer	5.85-6.3	0-0.11	0.21/0.034
G Pearl	2.7-3.05	0.04-0.16	0.22/0.008	N Metallic	3.2-3.4	0.08-0.15	0.17/0.005	U Clear coat	2.27-2.7	0.02-0.07	0.22/0.0049

The calculated transmissivity and reflectivity as functions of the frequency are shown in Fig. 9 (a) and (b), respectively. In this calculation, a paint layer with three-layer structure, as presented in Fig. 6 in [6], is considered, which is composed of primer, base coat and clear coat with thicknesses of 25 μm, 55 μm and 40 μm, respectively. Samples R and U are used as the layers of primer and clear coat. Various basecoat layers of solid, pearlescent and metallic blue as well as metallic silver which has a significant permittivity difference with other paints, are considered as the only variable in this calculation.

Transmissivity and reflectivity are functions of frequency, permittivity of material and thickness of paint layers [6]. Paint layers with solid and pearlescent basecoats have similar transmissivity and reflectivity. Slightly lower transmissivity and higher reflectivity are observed for the structure with metallic blue basecoat compared with the solid and pearlescent blue basecoat paint. Lower transmissivity is calculated for the metallic silver basecoat due to its higher dielectric loss. For multilayer structures with basecoats of the same color (blue) the calculated reflectivity shows the minimum within the frequency range of 0.6 THz—0.7 THz. For the metallic silver basecoat, however, the minimum of reflectivity is observed at 0.45 THz.

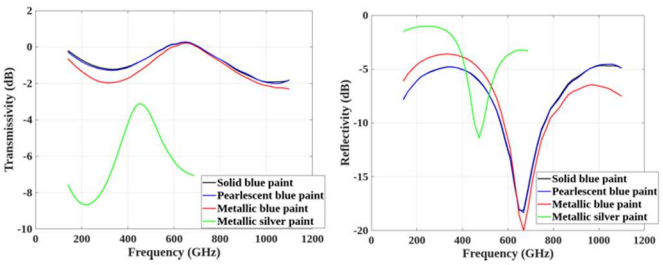

(a) (b)

Fig. 9 Calculated (a) transmissivity and (b) reflectivity of three layer paint having different basecoats.

The permittivity, and also reflectivity and transmissivity results that are shown in Fig. 9 can be used when automotive radar is mounted behind suitable vehicle components which are covered by paint layers.

V. Conclusion

In this paper, the CP of various automotive paints is investigated using VNA transmission setups. The measured permittivity values for three types of base coat samples in various colours, primer in three colours and clear coat are estimated and compared, and are utilized for further modelling of transmissivity and reflectivity of paint layers. The comparison between the measured CPs of various paints shows that metallic paints have higher imaginary parts of permittivity than other type of paints, and also, larger variation is observed from various samples of metallic paint whereas other type of paint show similar values for different samples. The modelling of various automotive paints showed higher transmissivity and lower reflectivity at some specific frequency ranges. These frequency ranges depend on the permittivity property of the materials and the thicknesses of mediums. For the silver metallic paint sample, the frequency band, where low reflectivity and high transmissivity are observed, differs from that of other paints due to the different CP value. The CP values of automotive paints obtained from this research is valuable for automotive industry to optimize radar placement behind suitable vehicle infrastructure with paint coatings. The feasibility of measuring CP using THz-VNA is explored and the measurement details are presented.

References

[1] R. Rasshofer and K. Gresser, "Automotive radar and lidar systems for next generation driver assistance functions," *Advances in Radio Science,* vol. 3, no. B. 4, pp. 205-209, 2005.

[2] M. Bekar, C. J. Baker, E. G. Hoare, and M. Gashinova, "Joint MIMO Radar and Communication System Using a PSK-LFM Waveform With TDM and CDM Approaches," *IEEE Sensors Journal,* vol. 21, no. 5, pp. 6115-6124, 2020.

[3] H.-L. Bloecher, A. Sailer, G. Rollmann, and J. Dickmann, "79 GHz UWB automotive short range radar–Spectrum allocation and technology trends," *Advances in Radio Science,* vol. 7, no. B. 3, pp. 61-65, 2009.

[4] F. Pfeiffer and E. M. Biebl, "Inductive compensation of high-permittivity coatings on automobile long-range radar radomes," *IEEE Transactions on Microwave Theory and Techniques,* vol. 57, no. 11, pp. 2627-2632, 2009.

[5] E. Emilsson, "Radar Transparency and Paint Compatibility-A Study of Automobile Bumper and Bumper-Skin Complex Permittivities for 77GHz Microwaves," Chalmers University of Technology, 2017.

[6] Y. Xiao, F. Norouzian, E. G. Hoare, E. Marchetti, M. Gashinova, and M. Cherniakov, "Modeling and Experiment Verification of Transmissivity of Low-THz Radar Signal Through Vehicle Infrastructure," *IEEE Sensors Journal,* vol. 20, no. 15, pp. 8483-8496, 2020.

[7] T. Tosaka, K. Fujii, K. Fukunaga, and A. Kasamatsu, "Development of complex relative permittivity measurement system based on free-space in 220–330-GHz range," *IEEE Trans. THz Sci. Technol.,* vol. 5, no. 1, pp. 102-109, 2015.

[8] M. Venkatesh and G. Raghavan, "An overview of dielectric properties measuring techniques," *Canadian biosystems engineering,* vol. 47, no. 7, pp. 15-30, 2005.

[9] L.-F. Chen, C. Ong, C. Neo, V. Varadan, and V. K. Varadan, *Microwave electronics: measurement and materials characterization*. John Wiley & Sons, 2004.

[10] I. Pupeza, R. Wilk, and M. Koch, "Highly accurate optical material parameter determination with THz time-domain spectroscopy," *Optics express,* vol. 15, no. 7, pp. 4335-4350, 2007.

[11] D. Ghodgaonkar, V. Varadan, and V. Varadan, "Free-space measurement of complex permittivity and complex permeability of magnetic materials at microwave frequencies," *IEEE Transactions on instrumentation and measurement,* vol. 39, no. 2, pp. 387-394, 1990.

[12] M. N. Sadiku, *Elements of electromagnetics*. Oxford university press, 2014.

[13] T. D. Dorney, R. G. Baraniuk, and D. M. Mittleman, "Material parameter estimation with terahertz time-domain spectroscopy," *JOSA A,* vol. 18, no. 7, pp. 1562-1571, 2001.

[14] Y. Dong, S. Lawman, Y. Zheng, D. Williams, J. Zhang, and Y.-C. Shen, "Nondestructive analysis of automotive paints with spectral domain optical coherence tomography," *Applied optics,* vol. 55, no. 13, pp. 3695-3700, 2016.

[15] K. Su, Y.-C. Shen, and J. A. Zeitler, "Terahertz sensor for non-contact thickness and quality measurement of automobile paints of varying complexity," *IEEE Transactions on Terahertz Science and Technology,* vol. 4, no. 4, pp. 432-439, 2014.

[16] https://www.keysight.com/en/pcx-x2015001/network-analyzers?nid=-32503.0&cc=GB&lc=eng.